Communication

Self-Assembled Hybrid Nanoparticles for Cancer-Specific Multimodal Imaging

Jason S. Kim, William J. Rieter, Kathryn M. L. Taylor, Hongyu An, Weili Lin, and Wenbin Lin

J. Am. Chem. Soc., **2007**, 129 (29), 8962-8963• DOI: 10.1021/ja073062z • Publication Date (Web): 30 June 2007

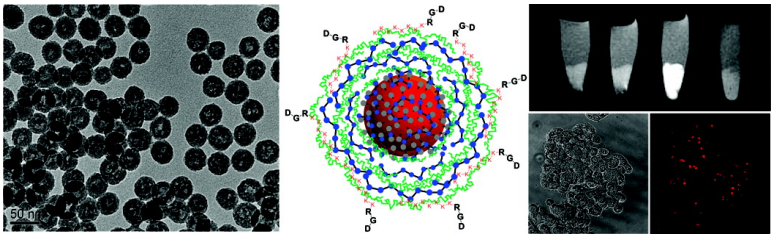

More About This Article

Additional resources and features associated with this article are available within the HTML version:

- Supporting Information
- Links to the 12 articles that cite this article, as of the time of this article download
- Access to high resolution figures
- Links to articles and content related to this article
- Copyright permission to reproduce figures and/or text from this article

View the Full Text HTML

J|A|C|S
COMMUNICATIONS

Published on Web 06/30/2007

Self-Assembled Hybrid Nanoparticles for Cancer-Specific Multimodal Imaging

Jason S. Kim,[†] William J. Rieter,[†] Kathryn M. L. Taylor,[†] Hongyu An,[‡] Weili Lin,[‡] and Wenbin Lin*,[†]

Departments of Chemistry and Radiology, University of North Carolina, Chapel Hill, North Carolina 27599

Received May 9, 2007; E-mail: wlin@unc.edu

Multifunctional nanoparticles (MFNPs) have shown great promise as new probes for biomedical imaging and carriers for drug delivery.[1] MFNPs can not only carry large payloads of imaging and/or therapeutic agents but also be rendered target-specific by conjugation to affinity molecules which have avidity for cell surface markers. Although a number of strategies have been developed to synthesize target-specific MFNPs, most of them rely on covalent attachment of affinity molecules to their surfaces.[2] Since such bioconjugation steps can be tedious, there exists a need for new synthetic strategies toward imaging and/or therapeutic MFNPs that can specifically target diseased cells. Herein we wish to report a noncovalent, electrostatic layer-by-layer (LbL) self-assembly strategy for the synthesis of cancer-specific MFNPs that are efficient contrast agents for multimodal imaging.

LbL self-assembly, which was first reported almost 25 years ago,[3] utilizes a wide range of interactions of varied strength, including covalent bonds,[4] metal−ligand coordination,[5] and electrostatic attractions between oppositely charged polyelectrolytes.[6] Whereas molecular self-assembly was initially developed for depositing monolayer and multilayer films on planar substrates, electrostatic LbL self-assembly of polyelectrolytes has recently been shown to be a versatile strategy for the synthesis of core−shell nanostructures and nanoshells.[7] In this work, we have prepared cancer-specific MFNPs by LbL self-assembly of polyelectrolytes and explored their in vitro applications in magnetic resonance (MR) and optical imaging.

Scheme 1 illustrates our LbL self-assembly strategy for MFNPs which were synthesized starting from recently reported hybrid silica nanoparticles (**NP0**) containing a luminescent $[Ru(bpy)_3]Cl_2$ core and a paramagnetic monolayer coating of the Gd−(siloxylpropyl)-diethylenetriamine tetraacetate (Gd−DTTA) complex.[8] **NP0** is a highly anionic nanoparticle owing to the negative charge on the Gd−DTTA complex and, as a result, allows the deposition of cationic Gd(III)−DOTA oligomer **1** via electrostatic interactions to afford **NP1A**. It has been shown that nanoparticles terminated with positively charged polyelectrolytes carry net positive charge to allow further deposition of anionic polymers via electrostatic interactions.[7] Treatment of **NP1A** with polystyrenesulfonate (PSS) yielded **NP1B** with a bilayer of **1** and PSS. Repetition of this LbL deposition sequence led to MFNPs with alternate multilayer coatings of positively charged **1** and negatively charged PSS. These MFNPs are designated **NP*n*A** or **NP*n*B** with ***n*** denoting the number of **1** or PSS coating and **A** and **B** denoting surface termination with **1** and PSS, respectively.

TEM images indicated alternate deposition of **1** and PSS onto the nanoparticles (Figure 1a−c); the average diameters for **NP1A**, **NP3A**, and **NP6A** are 37 ± 1, 41 ± 1, and 43 ± 2 nm, respectively. As shown in Figure 1d, the average diameters of the nanoparticles linearly increased as more bilayers of **1** and PSS were deposited. To further probe alternate deposition of **1** and PSS, we have

Scheme 1

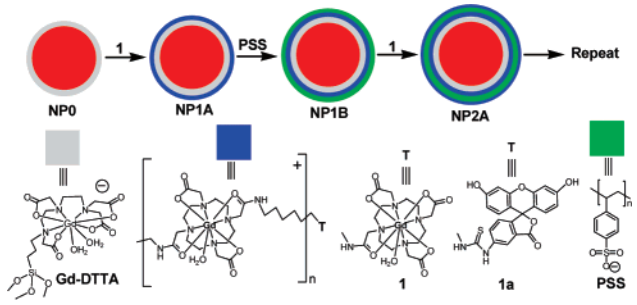

prepared a fluorescein isothiocyanate (FITC)-labeled cationic Gd−DOTA oligomer **1a**. Upon excitation at 488 nm, $[Ru(bpy)_3]Cl_2$-doped **NP0** emitted at 615 nm whereas the FITC dye emitted at 515 nm. Since the luminescence intensity at 615 nm is proportional to the **NP0** concentration, the ratio of the 515 nm emission intensity to 615 nm emission intensity is proportional to the number of FITC molecules on each nanoparticle. As shown in Figure 1e, the ratio between 515 nm emission and 615 nm emission increased quadratically as more layers of **1a** and PSS were deposited. This result is consistent with the linear increase of particle diameter since the number of FITC molecules is proportional to the surface area of spherical nanoparticles (which scales quadratically with the particle diameter).

We have determined longitudinal ($r1$) and transverse ($r2$) MR relaxivities for the LbL nanoparticles (**NP*n*A**) with up to seven layers of **1**. Interestingly, the relaxivity values for **NP*n*A** on a per Gd basis remain essentially constant at $r1 = 19.0 \pm 1.7$ $mM^{-1}\cdot s^{-1}$ and $r2 = 55.0 \pm 5.0$ $mM^{-1}\cdot s^{-1}$ regardless the number of deposited layers of **1**. This result is in stark contrast with that of the nanoparticles with covalently attached multilayers of Gd chelates

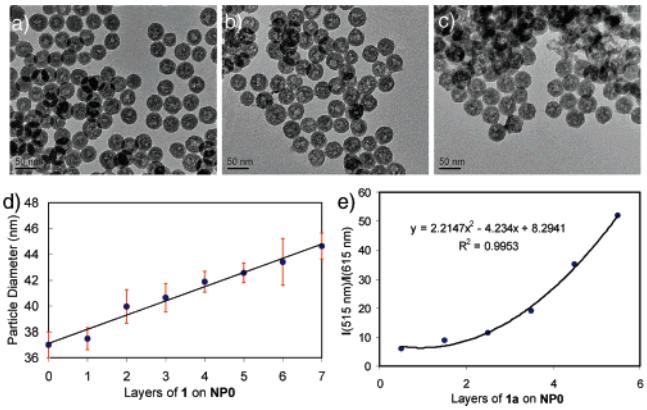

Figure 1. (a−c) TEM images of nanoparticles that have been terminated with cationic Gd−DOTA oligomer **1**: (a) **NP1A**; (b) **NP3A**; (c) **NP6A**. (d) Dependence of **NP*n*A** particle size on the number of deposited **1**. (e) Dependence of the intensity ratio between FITC (515 nm) and $[Ru(bpy)_3]Cl_2$ (615 nm) luminescence on the number of deposited FITC-labeled Gd−DOTA oligomer **1a**.

[†] Department of Chemistry.
[‡] Department of Radiology.

10.1021/ja073062z CCC: $37.00

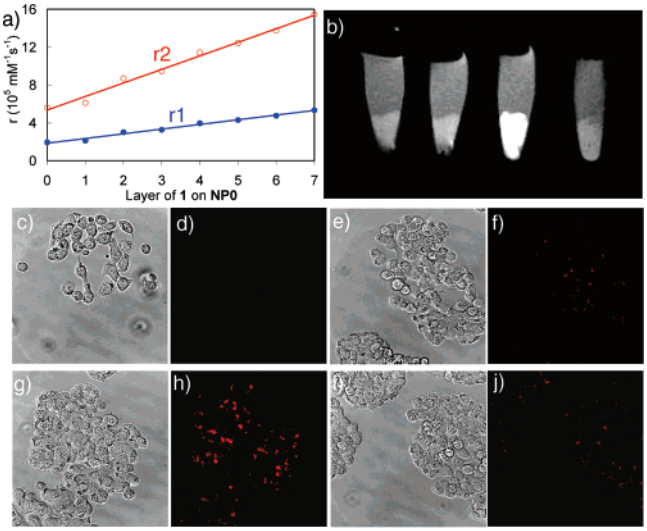

Figure 2. (a) Dependence of per particle *r*1 and *r*2 values on the number of deposited Gd−DOTA oligomer **1** on **NP0**. (b) *T*1-weighted MR images of HT-29 cells that have been incubated with various nanoparticles. From left to right: control cells without any nanoparticle, cells with **NP3B** particles, cells with **NP3B** particles that have been noncovalently functionalized with K_7RGD, and cells with **NP3B** particles that have been noncovalently functionalized with K_7GRD. (c−j) Phase contrast optical (c, e, g, and i) and LSCFM microscopic images (d, f, h, and j) of HT-29 cells that have been incubated with various nanoparticles: control cells without any nanoparticle (c and d), cells with **NP5B** particles (e and f), cells with **NP5B** particles that have been noncovalently functionalized with K_7RGD (g and h), and cells with **NP5B** particles that have been noncovalently functionalized with K_7GRD (i and j).

which exhibited diminished relaxivities on a per Gd basis.[8] We believe that the highly disordered and hydrophilic nature of **1** and PSS on **NP*n*A** allows ready accessibility of water molecules to the Gd centers for efficient water proton relaxation. On the basis of the size of LbL particles, we further estimated *r*1 and *r*2 relaxivities for **NP*n*A** on a per particle basis which increased linearly as more layers of **1** were electrostatically deposited onto **NP0** (Figure 2a). The per particle *r*1 values increase from 1.94×10^5 $mM^{-1}\cdot s^{-1}$ for **NP0** to 5.34×10^5 $mM^{-1}\cdot s^{-1}$ for **NP7A**, whereas the per particle *r*2 values increase from 5.61×10^5 $mM^{-1}\cdot s^{-1}$ for **NP0** to 1.55×10^6 $mM^{-1}\cdot s^{-1}$ for **NP7A**. The LbL self-assembly thus offers a superb strategy for increasing nanoparticle MR relaxivities.

Since LbL self-assembled nanoparticles (**NP*n*B**) are terminated with anionic PSS polymers, we hypothesized that **NP*n*B** can be further noncovalently functionalized with targeting peptides that carry positive charges under physiological conditions. A peptide sequence containing arginine-glycine-aspartate (RGD) and seven consecutive lysine (K) residues (K_7RGD) was chosen for this study. The negatively charged PSS layer can electrostatically interact with positively charged lysine residues of the K_7RGD sequence to lead to surface functionalization of **NP*n*B** particles with the RGD sequence. The RGD peptide is known to bind strongly (with a K_d in the micromolar range) to the integrin cell surface receptors that are upregulated in growing endothelial and angiogenic cancer cells.[9] We used human colon cancer (HT-29) cells and calf pulmonary artery endothelial (CPAE) cells for in vitro labeling studies. HT-29 cells are known to overexpress integrin receptors[10] and have been previously labeled with K_7RGD-functionalized protein microspheres.[11]

*T*1-weighted MR images of HT-29 cells after incubation with various nanoparticles are shown in Figure 2b. Significant signal enhancement in the *T*1-weighted image was observed only for HT-29 cells incubated with **NP3B** particles that have been noncovalently functionalized with the K_7RGD sequence. In contrast, no signal enhancement was observed for the HT-29 cells incubated with either **NP5B** particles or **NP5B** particles noncovalently functionalized with the K_7GRD sequence. The K_7GRD peptide was used here as a scramble to mimic the surface charge of the nanoparticles but without providing affinity for the integrin receptors. In vitro MR imaging studies demonstrated efficient targeting of cancer cells by the LbL particles with noncovalently attached K_7RGD peptide.

We have confirmed the targeting capability of LbL nanoparticles using laser scanning confocal fluorescence microscopic (LSCFM) imaging. As shown in Figure 2c−j, significant luminescent signal was observed for HT-29 cells incubated with **NP*n*B** particles that have been noncovalently functionalized with the K_7RGD sequence, indicating efficient targeting of HT-29 cells by the electrostatically attached K_7RGD peptide. In comparison, no or little luminescent signal was observed for control HT-29 cells without nanoparticles and for the cells that had been incubated with **NP5B** particles or **NP5B** particles noncovalently functionalized with the scrambled K_7GRD sequence. This result has been further supported by LSCFM studies of CPAE cells which also showed cell targeting by the **NP*n*B** particles with noncovalently attached K_7RGD peptide (Supporting Information).

In summary, we have utilized electrostatic LbL self-assembly to construct MFNPs with both MR and optical imaging capabilities. The LbL self-assembly strategy not only affords MFNPs with extraordinarily high MR relaxivities but also provides an efficient means for noncovalent functionalization of MFNPs with affinity molecules. The generality of this approach should allow the design of imaging and/or therapeutic MFNPs that can specifically target a wide range of diseased cells.

Acknowledgment. We acknowledge financial support from NIH (U54-CA119343 and P20 RR020764). We thank Dr. Aiguo Hu for providing **1** and **1a**, and Dr. Rihe Liu for access to his tissue culture facility. W.J.R. thanks NSF for a graduate fellowship, and W.L. is a Camille Dreyfus Teacher-Scholar.

Supporting Information Available: Experimental procedures and six figures. This material is available free of charge via the Internet at http://pubs.acs.org.

References

(1) (a) Bertin, P. A.; Gibbs, J. M.; Shen, C. K.-F.; Thaxton, C. S.; Russin, A.; Mirkin, C. A.; Nguyen, S. T. *J. Am. Chem. Soc.* **2006**, *128*, 4168. (b) McCarthy, J. R.; Kelly, K. A.; Sun, E. Y.; Weissleder, R. *Nanomedicine* **2007**, *2*, 153. (c) Torchilin, V. P. *Adv. Drug Delivery Rev.* **2006**, *58*, 1532. (d) Rhyner, M. N.; Smith, A. M.; Gao, X.; Mao, H.; Yang, L.; Nie, S. *Nanomedicine* **2006**, *1*, 209. (e) Morawski, A. M.; Lanza, G. A.; Wickline, S. A. *Curr. Opin. Biotechnol.* **2005**, *16*, 89. (f) Giri, S.; Trewyn, B. G.; Stellmaker, M. P.; Lin, V. S. *Angew. Chem., Int. Ed.* **2005**, *44*, 5038. (g) Hu, M.: Chen, J.; Li, Z. Y.; Au, L.; Hartland, G. V.; Li, X.; Marquez, M.; Xia, Y. *Chem. Soc. Rev.* **2006**, 1084.
(2) Hermanson, G. T. *Bioconjugate Techniques*; Academic Press: San Diego, CA, 1996.
(3) Nuzzo, R. G.; Allara, D. L. *J. Am. Chem. Soc.* **1983**, *105*, 4481.
(4) (a) Love, J. C.; Estroff, L. A.; Kriebel, J. K.; Nuzzo, R. G.; Whitesides, G. M. *Chem. Rev.* **2005**, *105*, 1103. (b) Lin, W.; Lin, W.; Wong, G. K.; Marks, T. J. *J. Am. Chem. Soc.* **1996**, *118*, 8034.
(5) Fang, M.; Kaschak, D. M.; Sutorik, A. C.; Mallouk, T. E. *J. Am. Chem. Soc.* **1997**, *119*, 12184.
(6) Decher, G. *Science* **1997**, *277*, 1232.
(7) (a) Schneider, G.; Decher, G. *Nano Lett.* **2004**, *4*, 1833. (b) Schneider, G.; Decher, G. *Nano Lett.* **2006**, *6*, 530. (c) Caruso, F.; Caruso, R. A.; Möhwald, H. *Science* **1998**, *282*, 1111. (d) Shchukin, D. G.; Sukhorukov, G. B.; Möhwald, H. *Angew. Chem., Int. Ed.* **2003**, *42*, 4472.
(8) Rieter, W. J.; Kim, J. S.; Taylor, K. M. L.; An, H.; Lin, W.; Tarrant, T.; Lin, W. *Angew. Chem., Int. Ed.* **2007**, *46*, 3680.
(9) (a) Folkman, J. *Nat. Med.* **1995**, *1*, 27. (b) Folkman, J. *N. Engl. J. Med.* **1995**, *333*, 1757.
(10) Lee, J. W.; Juliano, R. L. *Mol. Biol. Cell* **2000**, *11*, 1973.
(11) Toublan, F. J.-J.; Boppart, S.; Suslick, K. S. *J. Am. Chem. Soc.* **2006**, *128*, 3472.

JA073062Z